Journal of Physics: Conference Series **2767** (2024) 052013 doi:10.1088/1742-6596/2767/5/052013

Simulation of a conventionally neutral boundary layer with two-equation URANS

M Baungaard[1,2], M P van der Laan[1], M Kelly[1] and E L Hodgson[1]

[1]Technical University of Denmark, DTU Wind and Energy Systems, Risø Campus, Frederiksborgvej 399, 4000, Roskilde, Denmark.
[2]University of Oxford, Department of Engineering Science, Parks Road, Oxford OX1 3PJ, UK.

E-mail: plaa@dtu.dk

Abstract. Simulating conventionally neutral boundary layers (CNBLs) with the unsteady Reynolds-Averaged Navier-Stokes (URANS) technique is investigated in this paper using a modified two-equation linear eddy viscosity turbulence model. For CNBLs over a flat and uniform surface, as typically used as the inflow to wind farm simulations, the governing equations of URANS can be solved with a one-dimensional solver, which makes the simulation of a typical CNBL five to six orders of magnitude faster than with large-eddy simulation (LES) approaches. However, URANS on the other hand requires more modelling than LES, and its accuracy is heavily dependent on the turbulence model employed. Through a cross-code study of a CNBL case with data from five different LES codes, it is found that the length-scale limiter of the employed turbulence model should be removed to correctly predict the atmospheric boundary layer (ABL) height evolution and the qualitative shape of various atmospheric profiles. A parametric study of simulations with varying initial ABL height further demonstrates the prediction capabilities of URANS, although a comparison with LES data shows that modelling of turbulence anisotropy and near-surface turbulence could be improved.

1. Introduction

The parametrization of the atmospheric boundary layer (ABL) is a key component in simulations of wind farm flows, because it affects the operation of the wind turbines and the evolution of their wakes. In recent years, the conventionally neutral boundary layer (CNBL) has emerged as a popular atmospheric model for large-eddy simulations (LESs) of wind farm flows [1, 2] because it includes the effects of wind veering and the ABL top, which become increasingly important as wind turbines grow in size. Furthermore, the ABL top is important to include in wind farm simulations as it can affect the wind farm efficiency significantly [3]. Finally, the CNBL can often be observed at sea and is therefore especially relevant for offshore wind farm studies.

As described in the previous paragraph, the CNBL has some desirable physical features, but it also comes with some complications from a computationally point of view. First, it requires an additional equation for the potential temperature, which acts as an active scalar due to its two-way coupling with the momentum equation and which can potentially deteriorate the numerical stability of the solver. Second, in contrast with the commonly simulated neutral atmospheric surface layer (ASL) and pressure-driven boundary layer (PDBL), there will inevitably be a temporal evolution of the flow statistics due to the vertical heat flux gradient associated with the CNBL, which means that this type of flow is not well-suited for steady-state simulations. Either unsteady Reynolds-averaged Navier-Stokes (URANS) or LES are therefore the most

natural choices for simulating the CNBL. Nevertheless, there have also been attempts to model the CNBL with steady-state RANS, through simplifications such as prescription of a static temperature profile [4].

The focus of this paper is on URANS simulations of the CNBL, which has not been explored much in the literature. For horizontally homogeneous flow, e.g., flow over flat terrain with uniform roughness and no turbines, a clear advantage of URANS is that it can be simulated with a one-dimensional solver. In contrast, LES must use a three-dimensional solver to capture the important mechanism of vortex stretching, and furthermore its domain needs to be large enough to encompass ABL-filling flow structures; hence it is several orders of magnitude more computationally expensive compared to URANS. On the other hand, URANS requires more extensive parameterization of the turbulent flow, and the results can be sensitive to the choice of turbulence model. A variant of the two-equation k-ε model [5] is investigated in this study and compared to various LES data to assess its performance for CNBL simulations.

The numerical solver and setup will be briefly described in Sec. 2. A cross-code comparison will then be made in Sec. 3 for the "n04" CNBL case from Pedersen et al. (2014) [6], which is one of the most widely used CNBL test cases in the literature. To further test the generality of the URANS model, we subsequently consider additional cases with varying ABL height and compare with LES data from a recent database of CNBLs [3] in Sec. 4. Finally, the conclusions from the paper are summarized in Sec. 5.

2. Numerical solver and setup

In this paper we consider CNBLs over uniform and flat terrain, hence the ensemble-averaged mean flow is assumed to be horizontally homogeneous, which allows a 1D (single column) formulation of the governing incompressible URANS equations [7]:

$$\frac{\partial U}{\partial t} = f_\mathrm{c}(V - V_\mathrm{g}) - \frac{\partial \overline{u'w'}}{\partial z}, \tag{1}$$

$$\frac{\partial V}{\partial t} = f_\mathrm{c}(U_\mathrm{g} - U) - \frac{\partial \overline{v'w'}}{\partial z}, \tag{2}$$

$$\frac{\partial \Theta}{\partial t} = -\frac{\partial \overline{\theta'w'}}{\partial z}, \tag{3}$$

$$\frac{\partial k}{\partial t} = \underbrace{-\overline{u'w'}\frac{\partial U}{\partial z} - \overline{v'w'}\frac{\partial V}{\partial z}}_{\mathcal{P}} - \varepsilon + \underbrace{\frac{g}{\theta_0}\overline{\theta'w'}}_{\mathcal{B}} + \frac{\partial}{\partial z}\left(\frac{\nu_t}{\sigma_k}\frac{\partial k}{\partial z}\right), \tag{4}$$

$$\frac{\partial \varepsilon}{\partial t} = C^*_{\varepsilon 1}\frac{\varepsilon}{k}\mathcal{P} - C_{\varepsilon 2}\frac{\varepsilon^2}{k} + C_{\varepsilon 3}\frac{\varepsilon}{k}\mathcal{B} + \frac{\partial}{\partial z}\left(\frac{\nu_t}{\sigma_\varepsilon}\frac{\partial \varepsilon}{\partial z}\right), \tag{5}$$

$$\overline{u_i'u_j'} = -\nu_t\left(\frac{\partial U_i}{\partial x_j} + \frac{\partial U_j}{\partial x_i}\right) + \frac{2}{3}k\delta_{ij} \tag{6}$$

$$\overline{\theta' u_i'} = -\frac{\nu_t}{\mathrm{Pr}_t}\frac{\partial \Theta}{\partial x_i} \tag{7}$$

$$\nu_t = C_\mu \frac{k^2}{\varepsilon} \tag{8}$$

where U is the x-component of the mean flow, V is the y-component of the mean flow, z is the vertical coordinate, f_c is the Coriolis parameter, $(U_\mathrm{g}, V_\mathrm{g})$ is geostrophic wind vector, Θ is the mean potential temperature, θ_0 is the potential temperature profile of the hydrostatic background state (it is convenient to choose an isentropic background atmospheric state, because θ_0 is then constant with height, see [7]), g is the magnitude of the gravitational acceleration vector, k is the turbulent kinetic energy (TKE), ε is the dissipation of TKE, $\overline{u_i'u_j'}$ is the Reynolds

stress tensor, $\overline{\theta' u_i'}$ is the heat flux vector, ν_t is the eddy viscosity and the remaining symbols represent model constants. Flat terrain is used, hence the mean flow is parallel to the ground, i.e., $W = 0$, and no equation for W-momentum is solved. The k-ε turbulence model of Koblitz et al. (2015) [5] (adopted from Sogachev et al., 2012 [8]) is used, which has four specific traits compared to the standard k-ε model:

(i) $C^*_{\varepsilon 1}$ is *not* a constant (hence the asterisk), but is formulated to limit the turbulence length scale to some maximum value, $\ell_{\max}$, as adopted from Apsley & Castro (1997) [9]:

$$C^*_{\varepsilon 1} = C_{\varepsilon 1} + (C_{\varepsilon 2} - C_{\varepsilon 1}) \frac{C_\mu^{3/4} k^{3/2}}{\varepsilon \ell_{\max}}. \tag{9}$$

In this study, we consider two different settings of $\ell_{\max}$:

(a) Setting it to the Mellor-Yamada lengthscale, $\ell_{\max} = \ell_{\mathrm{MY}} = 0.075 \frac{\int_0^\infty z k^{1/2} dz}{\int_0^\infty k^{1/2} dz}$, as was used by Koblitz et al. (2015) [5].

(b) Setting $\ell_{\max} \to \infty$ corresponding to a constant $C^*_{\varepsilon 1} = C_{\varepsilon 1}$.

(ii) $C_{\varepsilon 3}$ is made a function of the local flux Richardson number, $\mathrm{Ri}_f = -\mathcal{B}/\mathcal{P}$, and $\ell_{\max}$. See details in paper of Koblitz et al. [5].

(iii) The turbulent Prandtl number, Pr_t, is reduced in unstable conditions, while it is constant for stable and neutral conditions. As there are no unstably stratified regions in CNBLs, $\mathrm{Pr}_t = 0.74$ throughout this study.

(iv) The model constants are tuned for atmospheric flows, see table 1.

While Koblitz et al. (2015) [5] tested their k-ε model on different cases, including over complex terrain, it was never applied to simulate a CNBL and its performance on this specific type of ABL is therefore the subject of this paper.

Table 1. Model constants for the k-ε model of Koblitz et al. (2015) [5].

C_μ	κ	$C_{\varepsilon 1}$	$C_{\varepsilon 2}$	σ_k	σ_ε
0.03	0.4	1.52	1.833	2.95	2.95

A rough wall boundary condition (BC) is used at the bottom of the domain, see Sørensen et al. (2007) [10] for details, while a symmetry BC is used at the top of the domain. The equations are solved with the in-house 1D finite-volume computational fluid dynamics (CFD) code, EllipSys1D [11], which discretizes the diffusion terms with second-order central differences and advances the flow in time with an implicit Euler scheme. The timestep used is $\Delta t = 1\,\mathrm{s}$ with a variable number of subiterations per timestep based on a residual criterion, while the grid is uniform with spacing $\Delta z = 7.5\,\mathrm{m}$ for $z < 750\,\mathrm{m}$ and is slightly stretched from $z = 750\,\mathrm{m}$ to the top of the domain at $z = 1000\,\mathrm{m}$.

LES is also conducted for the cross-code comparison in Sec. 3 using the same finite-volume solver as for the URANS simulations, although in a three-dimensional version instead, EllipSys3D [12]. The LES setup is the same as was used in a recent cross-code study by Hodgson et al. (2023) [13] and details about the numerical setup can be found there. One difference in the setup is however that a slightly different grid is used: The domain size is $L_x \times L_y \times L_z = 2.56\,\mathrm{km} \times 2.56\,\mathrm{km} \times 1.0\,\mathrm{km}$ with horizontal grid spacing $\Delta x = \Delta y = 10\,\mathrm{m}$, while the vertical grid spacing is the same as in the URANS. A timestep of $\Delta t = 1.0$ s is again used, which, for the case considered, ensures that the Courant-Friedrichs-Lewy (CFL) number is approximately equal to or less than one throughout the entire domain.

3. Cross-code validation

The "n04" CNBL case from Pedersen et al. (2014) [6] is used as the first test case, because it has also been used in several other LES studies, so abundant reference data exist; see table 2.

Table 2. Reference data for the "n04" case.

Short name	Authors
NCAR	Pedersen et al. (2014) [6]
WiRE	Abkar and Porte-Agel (2013) [14]
SP-Wind	Allaerts (2016) [15]
TOSCA	Stipa et al. (2024) [16]
E3D	New LES conducted with EllipSys3D for the current study.

The parameters and initializations for the "n04" case are summarized in table 3 and are identical to the ones used by Pedersen et al. (2014) [6].

Table 3. Initialization and parameters for the n04 case.

Variable	Value
Initial velocity profile	$U_{i,\text{initial}} = (U_\text{g}, V_\text{g}, 0)$
Initial potential temperature profile	$\Theta_\text{initial} = \theta_0 + \Gamma z + \theta_\text{pertub}(z)$
Geostrophic wind components	$U_\text{g} = 10$ m/s, $V_\text{g} = 0$ m/s
Roughness length	$z_0 = 0.01$ m
Coriolis parameter	$f_\text{c} = 10^{-4}$ s^{-1}
Free-atmosphere lapse rate	$\Gamma = 10$ K km^{-1}
Background temperature	$\theta_0 = 290.0$ K
Total simulation time	$\Delta t_\text{tot} = 24.0$ hr
Statistics averaging window	$t \in [23.0, 24.0]$ hr after start

Some sinusoidal pertubations, $\theta_\text{pertub}(z)$, are added to the initial potential temperature profile for $z < 100$ m in our LES to trigger turbulence. These pertubations are not included in our URANS simulations, because the turbulence is instead initialized via k and ε:

$$k_\text{initial} = \max\left\{0.4\left(1 - \frac{z}{h_0}\right)^3, 10^{-5}\right\} \text{ m}^2\text{s}^{-2}, \tag{10}$$

$$\varepsilon_\text{initial} = k_\text{initial}\tau_\text{initial}, \tag{11}$$

where we choose $h_0 = 250$ m and an initial turbulence time scale of $\tau_\text{initial} = 1$ s at all heights. This choice of URANS turbulence initialization has also been used in other ABL studies [17, 18, 19]. However, the effect of the turbulence initialization on the final results is nevertheless small compared to the choice of the potential temperature initialization [19].

The resulting ABL profiles of our LES and URANS simulations are shown together with the reference LES data in Fig. 1. Comparing the five LESs first, the overall trends are similar, but there are also some notable differences, especially in the potential temperature and second-order moment profiles. It is visible that our LES, simulated with EllipSys3D, has a slightly larger ABL height, which has also earlier been observed for a different CNBL case with our code [13]. The two URANS simulations both show relatively good agreement with the LES data, but the

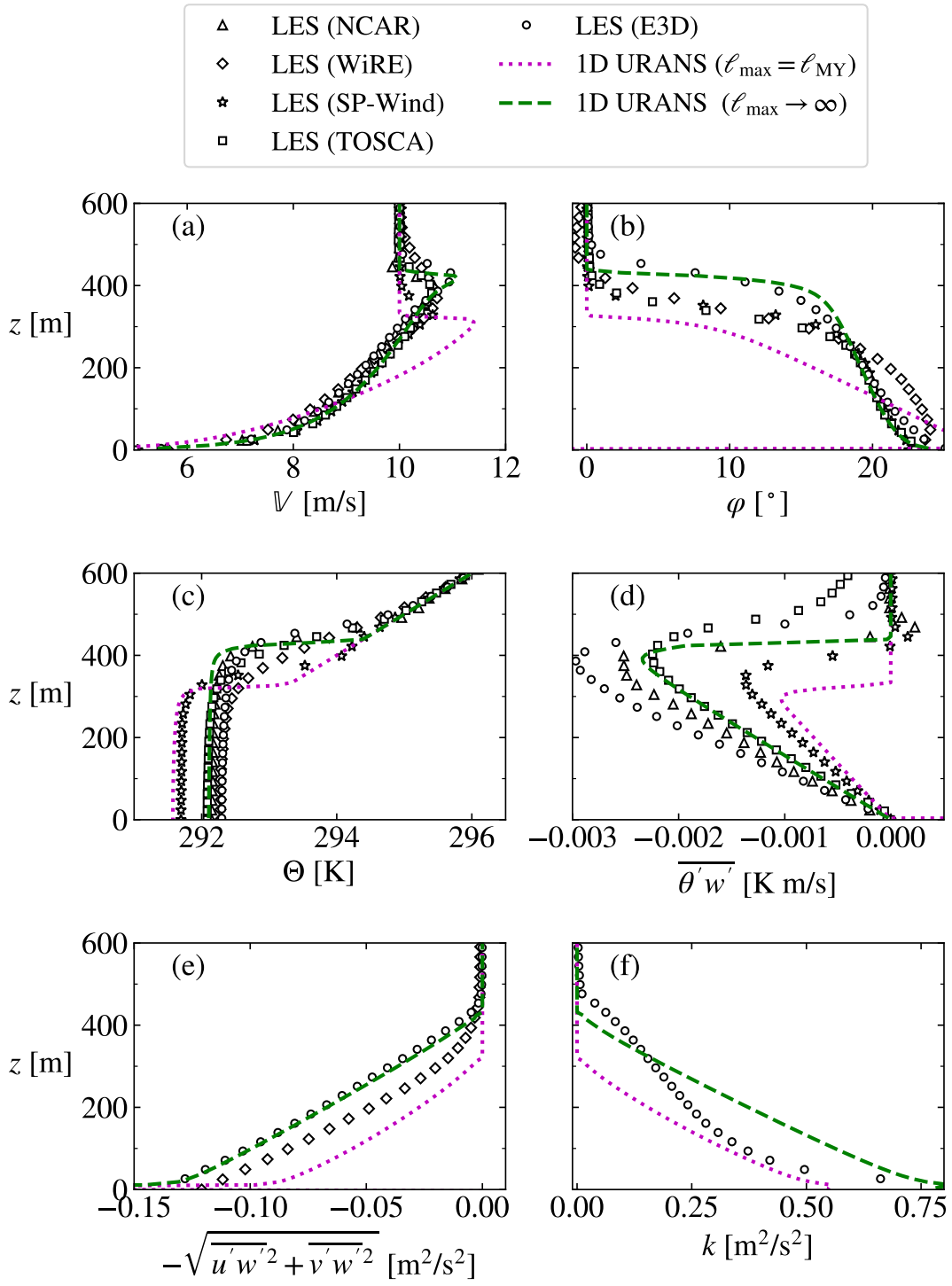

Figure 1. ABL profiles. (a) Wind speed, (b) wind direction, (c) potential temperature, (d) vertical heat flux, (e) total horizontal momentum flux and (f) turbulent kinetic energy.

URANS ($\ell_{max} \to \infty$) simulation is overall to be preferred. This indicates that a turbulence length scale limiter is *not* necessary for CNBLs when using an active temperature equation and that using $\ell_{max} = \ell_{MY}$ in fact erroneously double-counts the effect of the capping inversion on

the ABL.

One might object that the significantly smaller ABL height of the URANS ($\ell_{\max} = \ell_{\mathrm{MY}}$) simulation is because that the simulation has not yet reached a quasi-stationary state and still is evolving in time. Indeed, Fig. 2 shows that the ABL height[1], h, is still evolving (notice that the friction velocity, u_*, reaches a steady level much sooner than h and therefore the former is *not* an appropriate measure of whether an ABL has reached a quasi-stationary state), but it would take many days to reach the same ABL height because of its small dh/dt. Under any circumstance, the goal of a URANS model is not only to obtain the correct quasi-stationary state, but also to predict the correct transient behaviour, which the the URANS ($\ell_{\max} = \ell_{\mathrm{MY}}$) simulation clearly fails in this case.

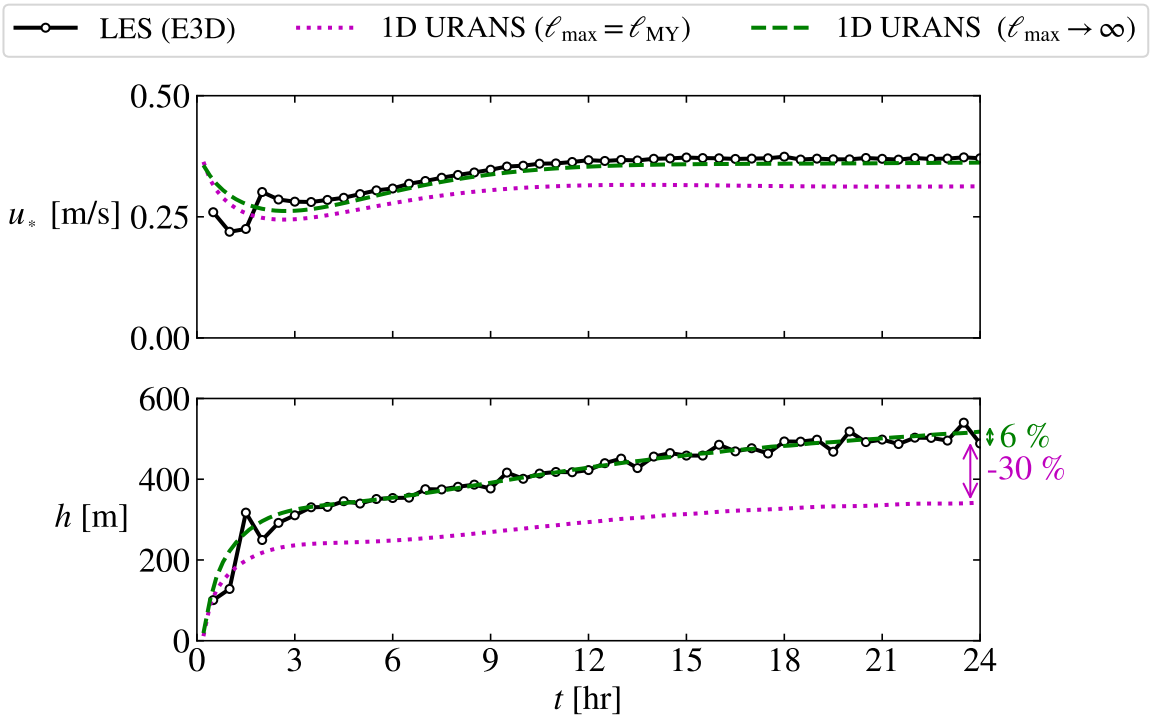

Figure 2. Time evolution of (top) friction velocity and (bottom) ABL height.

One clear fallacy of any variant of the k-ε model is that it predicts isotropic turbulence in horizontally homogeneous flows, i.e., $\overline{u'u'} = \overline{v'v'} = \overline{w'w'} = \frac{2}{3}k$, which is physically incorrect as is shown in Fig. 3. This consequently leads to an incorrect prediction of the TKE, because it is composed of the sum of the normal stresses, which could be part of the explanation of the difference between the URANS and LES profiles of TKE in Fig. 1. Another reason for the URANS overprediction of TKE near the surface could be an eddy viscosity coefficient, C_μ, that is too low, as will be discussed more in the next section.

4. Parametric study of ABL height

To asses the generality of the URANS ($\ell_{\max} \to \infty$) model, we will next consider some additional CNBL cases from the LES database of Lanzilao & Meyers (2024) [3]. The three specific cases

[1] The ABL height is obtained at each time instant through a curve fit to the expression $\sqrt{\overline{u'w'}^2 + \overline{v'w'}^2}/u_*^2 = \max\left\{(1 - z/h)^{2/3}, 0\right\}$ as suggested by Liu et al. (2021) [20].

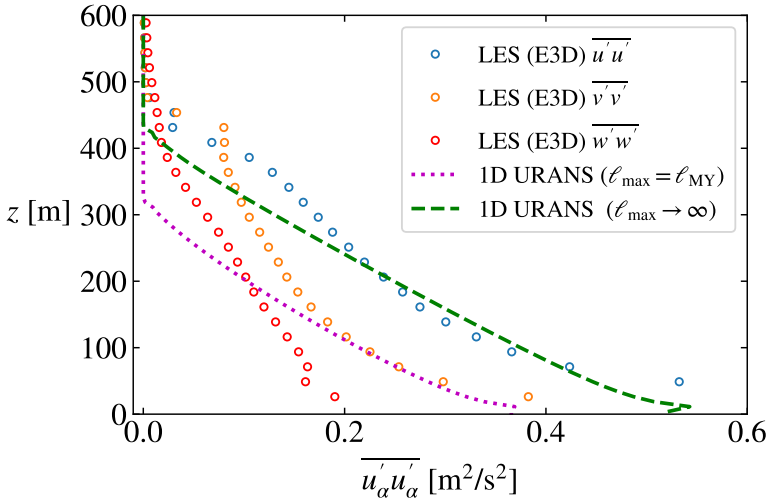

Figure 3. Normal stresses for the n04 case.

chosen from the database are given in table 4 and were chosen because they represent three commonly observed ABL heights for CNBLs.

Table 4. Case name and initial ABL height, h_0. Initial ABL height, "H"=h_0, capping-inversion strength, "C"=$\Delta\theta$ and free-atmosphere lapse rate, "G"=Γ.

Case name	h_0 [m]
H150-C2-G4	150
H300-C2-G4	300
H500-C2-G4	500

The horizontal velocity components are initalized using a Zilitinkevich model [21, 2], while the potential temperature is initialized with the Rampanelli & Zardi (2004) [22] model, see Appendix A, where the common parameters of the cases are also given. The main motivation of using these more advanced initialization profiles is to faster reach a quasi-stationary state of the CNBL. For the k and ε initialization in the URANS simulations, we use the same profiles as in the previous section, c.f., Eq. 10-11. All three cases use the parameters in table A1 and are run for $\Delta t_{\text{tot}} = 20$ hr with statistics gathered over the last four hours.

As is clear from Fig. 4, URANS is able to correctly predict the trends for all three LES cases. It is notable that the surface momentum flux is the same for all simulations, which however is to be expected, because all three cases have the same surface Rossby number, $\text{Ro} = G/(z_0|f_c|)$, and Zilintinkevich number, $\mu_N = N/|f_c| = \sqrt{\frac{g}{\theta_m}\Gamma}/|f_c|$ [23]. One striking difference between the URANS simulations and LESs is that the former overpredict the surface TKE by a significant amount. Since the momentum flux is correctly predicted by URANS and that the lower part of the ABL can be assumed to be in TKE equilibrium ($\mathcal{P}/\varepsilon = 1$), this indicates that the eddy viscosity coefficient should be larger to match the LES results. The implied eddy viscosity coefficient of the LESs is approximately

$$C_\mu^{\text{LES}} = \left(\frac{u_*^2}{k(z=0)}\right)^2 \approx 0.078, \tag{12}$$

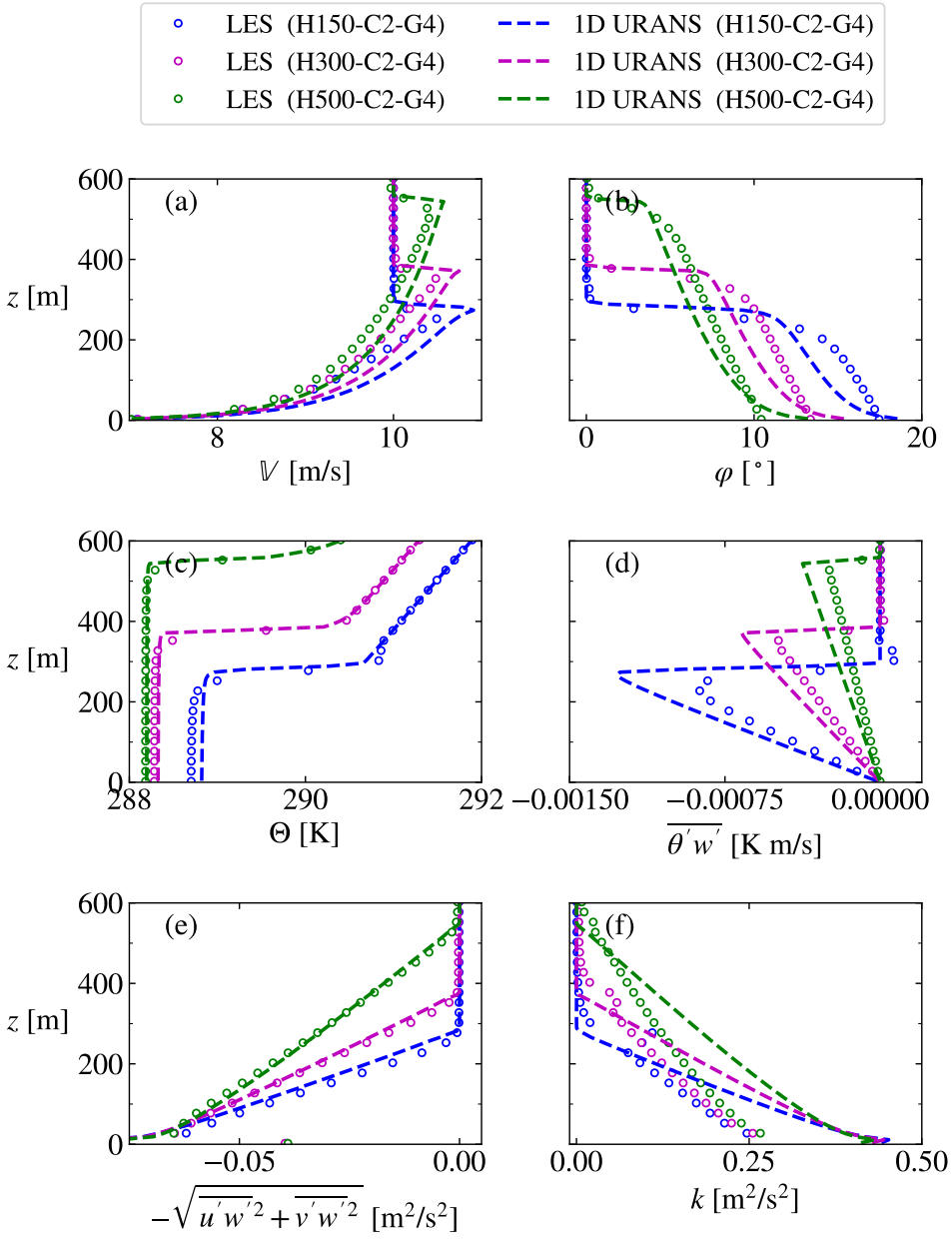

Figure 4. Same variables as Fig. 1, but for the Lanzilao & Meyers cases.

which is larger than the value of $C_\mu = 0.03$ used in our current URANS simulations and there is indeed a disagreement in the literature regarding this specific model constant, see review by Richards & Norris (2019) [24]. If one changes C_μ, one must however also change one (or more) of the other turbulence model constants to satisfy the log-law relation, thereby making the re-calibration process somewhat intricate. Such a re-calibration is therefore deferred to future studies.

5. Conclusions

The k-ε model variant of Koblitz et al. (2015) [5] has been tested for URANS simulations of the CNBL, which has become a popular type of ABL for the inflow to wind farm simulations.

Its performance is assessed by comparison with various LES data, both from the literature and a new LES, which have detailed flow descriptions of the CNBL (e.g., first- and second-order statistics at all heights and time history of ABL height) compared to currently available experimental data in the literature. For the first test case, the n04 CNBL case from Pedersen et al. (2014) [6], LES data is available from five different codes and it is immediately clear that, even among these expensive simulations, there is some spread in the results, especially for the second-order moments and the potential temperature profiles. Although the URANS simulation with the Koblitz et al. k-ε model qualitatively replicates the atmospheric profile shapes of the LESs, there is a clear tendency for it to underpredict the ABL height. Removing the length-scale limiter (equivalent to setting $\ell_{\max} \to \infty$) is found to amend this problem and the error in ABL height at the end of the simulation for this specific case was thereby reduced from 30% to 6%.

Next, three additional CNBL cases with different ABL heights were considered and again the atmospheric profile shapes of the URANS simulations are found to qualitatively match the LES data, except for the TKE profiles, where a clear overprediction occurs near the surface, presumably connected to the choice of eddy viscosity coefficient, $C_\mu = 0.03$, in the Koblitz et al. model. Another deficiency of the Koblitz et al. k-ε model is its incapability to predict anisotropic turbulence, which motivates the use of for example explicit algebraic Reynolds stress models in future studies. Nevertheless, since the main features of the ABL flow can be predicted and the URANS precursor generation is extremely fast due to its 1D formulation (for the n04 case, the URANS took ~ 25 core-seconds to simulate, while the LES took ~ 4500 core-hours), the model remains of interest to be tested for full 3D URANS wind farm simulations in future studies. Since the precursor generation constitutes a significant part of the computational effort for wind farm flow simulations, URANS simulations could be relevant to a broader audience including those that do not have access to large HPC clusters.

Acknowledgments
We gratefully acknowledge the computational and data resources provided on the Sophia HPC Cluster at the Technical University of Denmark [25]. The work has been supported by DTU and the Carlsberg Foundation (grant CF23-1002). We would also like to thank Luca Lanzilao for sharing the LES data used in Sec. 4.

Appendix A. Velocity and potential temperature initialization for the Lanzilao & Meyers CNBL cases

Zilintinkevich velocity profile [21, 2]:

$$U_{\text{zil}} = U_\downarrow \frac{1-\tanh(\psi)}{2} + U_\uparrow \frac{1+\tanh(\psi)}{2}, \tag{A.1}$$

$$V_{\text{zil}} = V_\downarrow \frac{1-\tanh(\psi)}{2} + V_\uparrow \frac{1+\tanh(\psi)}{2}, \tag{A.2}$$

$$U_\downarrow = \frac{u_*}{\kappa}\left(\log\left(\frac{z}{z_0}\right) + f_u\right) \quad , \quad U_\uparrow = G\cos(\alpha), \tag{A.3}$$

$$V_\downarrow = -\frac{u_*}{\kappa} f_v \,\text{sign}\,(f_v) \quad , \quad V_\uparrow = G\sin(\alpha), \tag{A.4}$$

where $\psi = (2\zeta - 1)h_0/\delta$, $\zeta = z/h_0$, $f_u = 1.57\zeta - 2.68\zeta^2$, $f_v = 13.2\zeta - 8.70\zeta^2$ and $\alpha = \arctan\left(V_\downarrow/U_\downarrow\right)|_{\zeta=1}$. One can rotate this profile to have a zero wind direction at any desired height – in this paper, we rotate the profile to have zero mean wind direction at the top of the domain, i.e., $U_{\text{g}} = G$ and $V_{\text{g}} = 0$ at $z = L_z$.

Rampanelli & Zardi (2004) [22] potential temperature profile:

$$\theta = \theta_m + a\frac{\tanh(\eta)+1}{2} + b\frac{\ln\left[2\cosh(\eta)\right]+\eta}{2}, \tag{A.5}$$

where $\eta = 3(z-l)/(\Delta h)$, $l = h_0 + \Delta h/2$, $b = \Gamma\Delta h/3$ and $a = \Delta\theta - b$.

See table A1, for the meaning of the different input parameters and the values used in the current study.

Table A1. Common parameters used in the current study for (left) the velocity initialization with the Zilintikevich model and (right) the temperature initialization with the Rampenelli & Zardi model. Identical to the values used by Lanzilao & Meyers (2024) [3].

Variable	Value
Geostrophic wind speed	$G = 10$ m/s
Roughness length	$z_0 = 10^{-4}$ m
Coriolis parameter	$f_c = 1.14 \cdot 10^{-4}$ s^{-1}
Initial friction velocity	$u_* = 0.26$ m/s
von Karman constant	$\kappa = 0.4$
Merging width	$\delta = 100$ m

Variable	Value
Capping inversion strength	$\Delta\theta = 2$ K
Free-atmosphere lapse rate	$\Gamma = 4$ K km^{-1}
Mixed-layer temperature	$\theta_m = 283.15$ K
Merging width	$\Delta h = 100$ m

References

[1] Churchfield M J, Lee S, Michalakes J and Moriarty P J 2012 *Journal of Turbulence* **13** 1–32
[2] Allaerts D and Meyers J 2015 *Physics of Fluids* **27** 065108
[3] Lanzilao L and Meyers J 2024 *Journal of Fluid Mechanics* **979** A54
[4] van der Laan M P, García-Santiago O, Kelly M, Meyer Forsting A, Dubreuil-Boisclair C, Sponheim Seim K, Imberger M, Peña A, Sørensen N N and Réthoré P E 2023 *Wind Energy Science* **8** 819–848
[5] Koblitz T, Bechmann A, Sogachev A, Sørensen N and Réthoré P E 2015 *Wind Energy* **18** 75–89
[6] Pedersen J G, Gryning S E and Kelly M 2014 *Boundary-Layer Meteorology* **153** 43–62
[7] Wyngaard J C 2010 *Turbulence in the atmosphere* (Cambridge University Press) ISBN 9780511840524
[8] Sogachev A, Kelly M and Leclerc M Y 2012 *Boundary-Layer Meteorology* **145** 307–327
[9] Apsley D D and Castro I P 1997 *Boundary-Layer Meteorology* **83** 75–98
[10] Sørensen N N, Bechmann A, Johansen J, Myllerup L, Botha P, Vinther S and Nielsen B S 2007 *Journal of Physics: Conference Series - Torque* **75** 012053
[11] van der Laan P and Sørensen N N 2017 A 1D version of EllipSys Tech. rep. Technical University of Denmark URL `https://orbit.dtu.dk/en/publications/a-1d-version-of-ellipsys`
[12] Sørensen N N 1995 *General purpose flow solver applied to flow over hills* Ph.D. thesis Technical University of Denmark URL `https://orbit.dtu.dk/en/publications/general-purpose-flow-solver-applied-to-flow-over-hills`
[13] Hodgson E L, Souaiby M, Troldborg N, Porté-Agel F and Andersen S J 2023 *Journal of Physics: Conference Series* **2505** 012009
[14] Abkar M and Porté-Agel F 2013 *Energies* **6** 2338–2361
[15] Allaerts D 2016 *Large-eddy simulation of wind farms in conventionally neutral and stable atmospheric boundary layers* Ph.D. thesis KU Leuven
[16] Stipa S, Ajay A, Allaerts D and Brinkerhoff J 2024 *Wind Energy Science* **9** 297–320
[17] Cuxart J, Holtslag A A, Beare R J, Bazile E, Beljaars A, Cheng A, Conangla L, Ek M, Freedman F, Hamdi R and et al 2006 *Boundary-Layer Meteorology* **118** 273–303
[18] Lazeroms W M, Svensson G, Bazile E, Brethouwer G, Wallin S and Johansson A V 2016 *Boundary-Layer Meteorology* **161** 19–47
[19] Želi V, Brethouwer G, Wallin S and Johansson A V 2021 *Boundary-Layer Meteorology* **178** 487–497
[20] Liu L, Gadde S N and Stevens R J 2021 *Physical Review Letters* **126** 104502
[21] Zilitinkevich S S 1989 *Boundary-Layer Meteorology* **46** 367–387
[22] Rampanelli G and Zardi D 2004 *Journal of Applied Meteorology* **43** 925–933
[23] Liu L, Gadde S N and Stevens R J 2021 *Quarterly Journal of the Royal Meteorological Society* **147** 847–857
[24] Richards P J and Norris S E 2019 *Journal of Wind Engineering and Industrial Aerodynamics* **190** 245–255
[25] Technical University of Denmark 2019 Sophia hpc cluster URL `https://dtu-sophia.github.io/docs/`